ChemComm

COMMUNICATION

View Article Online
View Journal | View Issue

Published on 08 September 2022. Downloaded by Wayne State University on 12/10/2022 2:50:15 AM.

Check for updates

Cite this: *Chem. Commun.*, 2022, **58**, 11260

Received 11th July 2022,
Accepted 7th September 2022

DOI: 10.1039/d2cc03872b

rsc.li/chemcomm

Quantum dot gels as efficient and unique photocatalysts for organic synthesis†

Daohua Liu,[a] James Nyakuchena,[b] Rajendra Maity,[a] Xin Geng,[a] Jyoti P. Mahajan,[a] Chathurange C. Hewa-Rahinduwage,[a] Yi Peng,[a] Jier Huang *[b] and Long Luo *[a]

Here we report CdS quantum dot (QD) gels as highly efficient and unique photocatalysts for organic synthesis. We found that the photocatalytic activity of CdS QD gel was superior to phosphine oxide- and thiolate-capped CdS QDs for dehalogenation and α-amine arylation reactions because of the high accessibility of its surface sites to the substrates. In addition, we discovered the unique reactivity of CdS QD gel for ring-opening during α-amine arylation of tetrahydroisoquinoline *via* the reductive cleavage of C–N bonds. QD gels provide new opportunities in photocatalysis due to their unique surface interactions with the substrates or intermediates.

Metal chalcogenide quantum dots (QDs), such as CdS and CdSe QDs, are an attractive group of photocatalysts for various chemical transformations, including water splitting,[1–3] CO_2 reduction,[4–6] N_2 reduction,[7] biomass valorization,[8] and organic synthesis.[9–13] Photocatalytic assessment of QDs is motivated by their unique photophysical and photochemical properties, such as the tunable redox potential by QD size, the large extinction coefficient, and the unique catalyst–substrate interface.[9,14,15] When colloidal QDs are used for photocatalytic organic synthesis, capping ligands are on the QD surface. Common ligands include oleates,[9] thiolates,[11] alkyl phosphines,[16] and alkylamines.[17] Except for stabilizing the QD catalysts in the reaction solution, surface ligands also strongly influence the permeability and accessibility of the substrates to active catalytic sites.[8,18]

QD gel is a 3-D connected pore-matter nanoarchitecture of interconnected QDs, prepared by electrochemical or chemical oxidation of thiolate-capped QDs.[19–21] Unlike QDs, QD gels lose most surface ligands during gelation but retain the quantum confinement characteristics of the QDs.[19] The similarities and differences between QDs and QD gels motivate us to investigate their photocatalytic activities. Fig. 1(a) illustrates the synthesis of CdS QD gel. The original trioctylphosphine oxide (TOPO) ligand is first exchanged with thioglycolic acid (TGA) to form TGA-capped CdS QDs. Then, thiolate ligands are oxidatively removed as disulfides, and CdS QDs are further oxidized to form interparticle dichalcogenide bonds between QDs during electrogelation, forming a QD network (Fig. S1, ESI†). Fig. 1(b)–(d) shows transmission electron microscopy (TEM) images and photographs of TOPO/CdS QDs, TGA/CdS QDs, and a CdS QD gel. The CdS QD gel has a crystallite size of ~3.2 nm like the TOPO/CdS and TGA/CdS QDs (Fig. S2 and S3, ESI†). All three

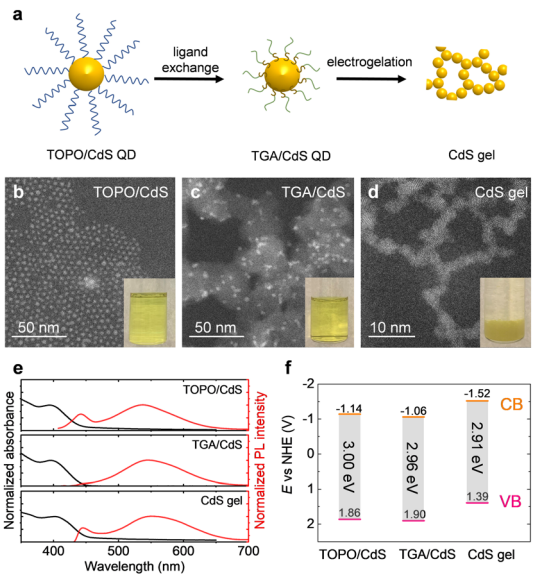

Fig. 1 (a) Schematic illustration of the transformation of TOPO-capped CdS QDs (TOPO/CdS) to TGA-capped CdS QDs (TGA/CdS) and a CdS QD gel. (b)–(d) Corresponding TEM images and photographs. (e) Normalized UV-Vis absorption spectra (black) and photoluminescence spectra (red). (f) Energy band positions. CB and VB stand for conduction and valence bands, respectively. Note: the TGA/CdS TEM sample was prepared by supporting the QDs on carbon due to its instability during sample preparation.

[a] *Department of Chemistry, Wayne State University, Detroit, Michigan 48202, USA. E-mail: long.luo@wayne.edu*

[b] *Department of Chemistry, Marquette University, Milwaukee, Wisconsin, 53201, USA. E-mail: jier.huang@marquette.edu*

† Electronic supplementary information (ESI) available. CCDC 2189462. For ESI and crystallographic data in CIF or other electronic format see DOI: https://doi.org/10.1039/d2cc03872b

This journal is © The Royal Society of Chemistry 2022

Published on 08 September 2022. Downloaded by Wayne State University on 12/10/2022 2:50:15 AM.

samples show a 1st exciton peak at ~395 nm (Fig. 1(e)), a weak band edge emission at 450 nm, and a dominant trap state emission at ~570 nm (Fig. 1(e)).[21] Their energy level diagrams show that the bandgap of the CdS gel remains unchanged, but its conduction and valence bands shift up by ~0.5 V relative to TOPO/CdS and TGA/CdS QDs (Fig. 1(f) and Fig. S4, ESI†) because of the ligand-induced surface dipole effect.[22]

First, we tested the photocatalytic performance of the CdS QDs and gel using the reductive dehalogenation of methyl 4-bromobenzoate as a model reaction (Fig. 2(a)). Fig. 2(b) illustrates the reaction mechanism supported by spectroscopic data in Fig. S5 (ESI†) and the literature report.[23,24] The blue light-excited CdS QDs oxidize tributylamine (Bu_3N, E = 0.68 V *vs.* NHE[25]), forming the radical anion of QDs or the gel (QD^-) and the radical cation of Bu_3N ($Bu_3N^{+\bullet}$). Then, QD^- transfers an electron to bromo-benzoate (E = −0.92 V *vs.* NHE[26]), yielding an aryl radical, which abstracts a hydrogen atom from $Bu_3N^{+\bullet}$ to form the dehalogenation product.[27] The reaction additive, formic acid, plays a role in the imine/enamine equilibrium.[27]

Fig. 2(c) shows the time-dependent debromination yield for the CdS QDs and gel with the same catalyst loading of 0.8 mmol% relative to the methyl 4-bromobenzoate substrate. In the absence of light or catalyst, we did not observe methyl benzoate formation (<1%). TOPO/CdS and TGA/CdS QDs produced a debromination yield of 32% and 64% in 5 hours under blue light irradiation. In comparison, the CdS gel exhibited much faster catalytic debromination (~10 to 20 times in the first hour) than the CdS QDs, and the reaction was completed in 3 hours.

Previous studies have shown that the charge transfer rate between colloidal QDs and substrates strongly depends on the substrate's permeability through the ligand shell and adsorbability to the QD core.[18] Since the QD gel has lost most of its surface ligands during electrogelation (Fig. S1, ESI†), we hypothesized that the superior photocatalytic activity of QD gel over QDs mainly arose from more exposed surface sites increasing the probability of either transiently or statically adsorbing reactants, promoting the charge transfer.

To test this hypothesis, we externally added 0.2 equiv. and 0.6 equiv. of TGA ligand, relative to the methyl 4-bromobenzoate substrate, to the reaction mixture with the CdS gel as the catalyst. The introduction of TGA nearly completely shut down the debromination reaction (Table S1, ESI†). To rule out the possibility of TGA competing with Bu_3N to react with holes, we also tested 0.2 equiv. of redox inert pyridine ligand.[28] Similar suppression of catalytic activity was observed (Table S1, ESI†), confirming the importance of the exposed surface sites of the QD gel in the reaction. Next, we performed femtosecond transient absorption spectroscopy (TA) measurements to study the interactions between Bu_3N and QDs or QD gel. Following 380 nm excitation, the TA spectra of the QDs and QD gel showed an exciton bleach band around 425 nm (Fig. S6, ESI†), consistent with the first exciton band as shown in Fig. 1. Fig. 3 compares

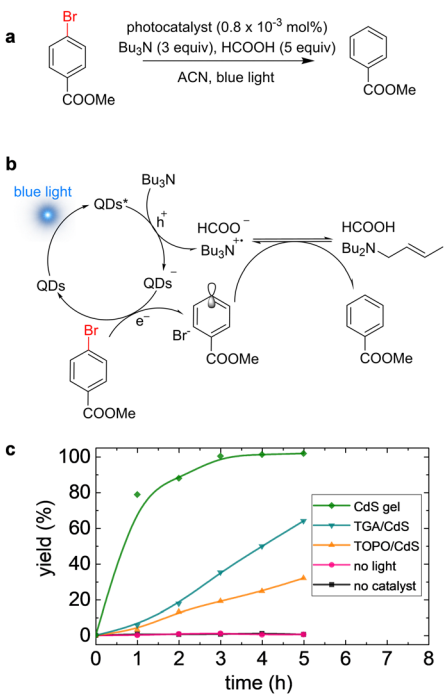

Fig. 2 (a) Reaction conditions and (b) proposed mechanism for photocatalytic dehalogenation of methyl 4-bromobenzoate using the CdS QDs and gel as the photocatalyst. (c) The time-dependent yield during dehalogenation of methyl 4-bromobenzoate under no light with the gel (pink), and under blue light with no catalyst (black), TOPO/CdS and TGA/CdS (orange and cyan) and the gel (green).

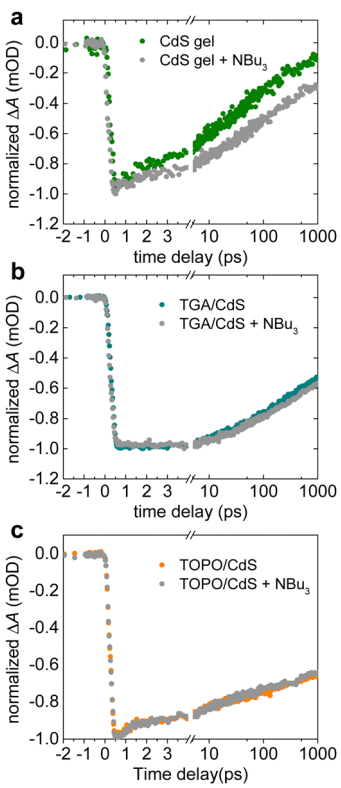

Fig. 3 Normalized transient absorption spectra of the bleach recovery with and without the addition of NBu_3 for (a) CdS gel, (b) TGA/CdS, and (c) TOPO/CdS in acetonitrile after 380 nm excitation.

Published on 08 September 2022. Downloaded by Wayne State University on 12/10/2022 2:50:15 AM.

their exciton bleach recovery kinetics in the absence and presence of Bu_3N. In the absence of Bu_3N, the bleach recovery kinetics follows the order of TOPO/CdS < TGA/CdS < gel (Fig. S7, ESI†). The slightly faster recovery of TGA/CdS relative to TOPO/CdS is because the charge transfer between the hole and redox-active TGA reduces the radiative recombination rate.[29] Likewise, the faster bleach recovery of the CdS gel can be attributed to surface traps associated with undercoordinated Cd surface sites. After adding Bu_3N, the TA spectra for the QD samples were essentially unchanged. However, the bleach recovery for the CdS gel became slower, indicating that Bu_3N can bind to and thereby passivate surface trap sites on the gel but not on TGA/CdS or TOPO/CdS.[30,31] The steady-state photoluminescence spectra of CdS gel shown in Fig. S8 (ESI†) also show the increasing band-edge emission with increasing Bu_3N addition, confirming the passivation of surface trap sites on the CdS gel by Bu_3N. The high accessibility of surface sites of the gel to Bu_3N promotes charge transfer and, thereby, the overall photocatalytic dehalogenation kinetics.

We also considered an alternative hypothesis that the more substantial reducing power of QD gel (−1.52 V) than ligand-capped QDs (∼−1.1 V) was responsible for the observed fast debromination for QD gel since the bromobenzoate reduction potential (−0.92 V) is close to that of the QDs (∼−1.1 V). To test it, we ran iodobenzoate reduction, which is thermodynamically easier than the bromobenzoate reduction due to the weaker C–I bond is than the C–Br bond. Fig. S9 (ESI†) shows that the deiodination reaction using CdS gel and TGA/CdS QDs approaches the scenario where catalyst loading is no longer the limiting factor, even at a low loading of 0.14×10^{-3} mol%. However, TOPO/CdS QDs still have the lowest activity among the three, despite their reducing powder being close to that of TGA/CdS QDs, suggesting that the ligands—at least the long ones—slow down the dehalogenation reaction.

Encouraged by the significantly improved dehalogenation activity of the CdS gel relative to QDs, we tested its applicability to other reactions. Fig. 4(a) shows an α-amino arylation reaction in which amine **1** is oxidized and dicyanobenzene **2** is reduced by a photocatalyst, followed by the cross-coupling of their radical products (Fig. S10, ESI†). Fig. 4(b) shows that the CdS gel also exhibits a much higher yield (82%) than TOPO/CdS and TGA/CdS QDs (38% and 58%, respectively) under the same reaction conditions, confirming that the catalytic activity improvement of CdS gel is not limited to the dehalogenation reaction. The gel catalyst is easily recyclable by centrifuging the reaction mixture. The recycled catalyst exhibited similar activity as the fresh catalyst, giving a yield of 70% for the arylated product, comparable with the yield of 82% using the fresh catalyst (Fig. 4(b)). We further explored the scope of amines and electron-deficient cyanoaromatics for this reaction. Pyrrolidines with different functional groups (**3a**–**3d**), piperazine (**3e**), 1,2-dicyanobenzene (**3f**), ethyl 4-cynobenzoate (**3g**), and 4-cyanopyridine (**3h**) all furnished the arylation product with moderate to high yields from 30% to 87%, comparable to the yields achieved using an Ir-based molecular photocatalyst.[32]

Two unexpected yet exciting findings were revealed during the substrate scope development. First, 11% of **4d** (the *ortho* isomer of **3d**) was formed using the CdS gel catalyst when the reaction was continued for another 3 h after **2** was consumed (Fig. 5(a) and Fig. S11, ESI†). The corresponding QDs also produced **4d**, but at lower yields. Such an isomerization reaction was not observed for other pyrrolidine substrates or when using Ir-based molecular photocatalysts. A similar rearrangement of aromatic and heteroaromatic systems was only reported before as ''halogen dance reactions'', which proceed *via* an aryl anion intermediate formed by metal–halogen exchange or through a deprotonation reaction using a strong base such as potassium amide and lithium diisopropylamide.[33] Thus, we suspect that a similar aryl anion was formed during the electron transfer between the ester-bearing substrate and the QDs or QD gel, and the surface interactions between the ester group and QD gel play an essential role in such an electron transfer. Second, we discovered that the CdS gel led to the ring-opening arylation of tetrahydroisoquinolines (THIQ) *via* the reductive cleavage of the C–N bond (Fig. 5(b))—reactivity that was not observed with the TGA/CdS QD photocatalyst. Transformation of THIQ *via* scission of the C–N bond is rare, and the reductive ring-opening arylation of THIQ has not been reported. According to the literature,[34–36] the ring-opening reactions of the THIQ skeleton typically involve a quaternary ammonium intermediate, formed by the reaction between amine and methyl iodide or a superacid such as triflic acid. The C–N bond is significantly weakened in the quaternary ammonium salts, allowing reductive cleavage. Therefore, we speculate that similar quaternary ammonium intermediates have formed due to the surface interaction between the QD gel and THIQ compounds. Our substrate scope results shown in Fig. 5(b) support this speculation because the electron-rich THIQs, whose

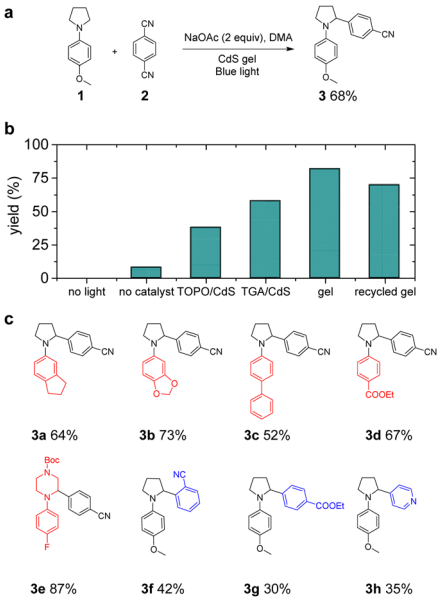

Fig. 4 (a) Photoredox catalytic α-amino arylation reaction conditions. (b) Arylation product yields under various conditions after 15 h. (c) Substrate scope. Reaction scale: 0.625 mmol amine, 0.5 mmol cyanoaromatics, and 2 mmol% CdS gel with respect to cyanoaromatics. Panels (a) and (c) show the isolated yields after reaction completion. Panel (b) shows the ^{1}H NMR yield using dichloromethane as an internal standard.

 This journal is © The Royal Society of Chemistry 2022

Published on 08 September 2022. Downloaded by Wayne State University on 12/10/2022 2:50:15 AM.

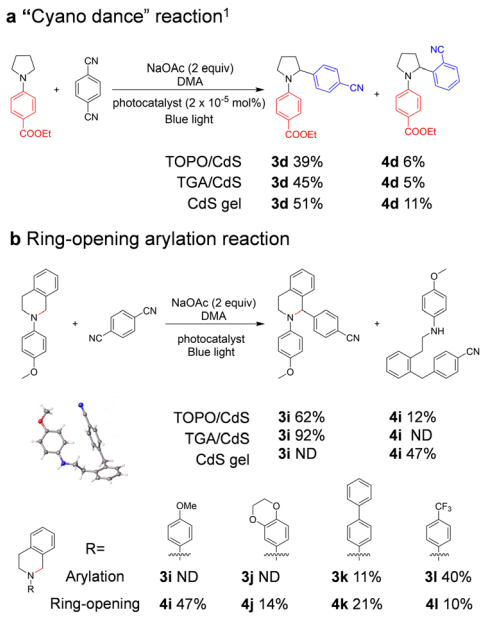

Fig. 5 (a) Cyano dance reaction and (b) reductive ring-opening arylation catalyzed by CdS QDs and gel. The inset on the lower left of panel (b) is the crystal structure of **4i**. Note 1: the reaction time is 9 h. For CdS gel, **2** was consumed and amine was not after 6 h of reaction time.

quaternary ammonium salts are better stabilized, are more prone to ring-opening than the electron-deficient ones (**4i** to **4l**). However, the detailed mechanisms for the ester group-enabled cyano dance and reductive ring-opening arylation of THIQ are still under investigation.

In conclusion, we have reported the photocatalytic activity of QD gels for dehalogenation and amine arylation reactions. Compared with TOPO- and TGA-capped CdS QDs with the same bandgap, CdS gels exhibited superior photocatalytic activity due to the removal of surface ligands during gel synthesis, which enables high accessibility of surface sites to substrates. We also discovered the unique activity of the CdS gel for the cyano dance reaction and the reductive ring opening arylation reaction of tetrahydroisoquinolines. QD gels provide new opportunities in photocatalysis due to their unique surface interactions with the substrates or intermediates.

D. L., J. P. M., and L. L. gratefully acknowledge support from NIH (1R35 GM142590-01), the start-up funds, and the Faculty Competition for Postdoctoral Fellows Award from Wayne State University. J. H. and J. N. acknowledge the support from Wehr Foundation and O'Brian Fellowship, respectively. This work used HRMS supported by NIH R01 GM098285-07S1. The authors thank S. L. Brock for proofreading.

Conflicts of interest

There are no conflicts to declare.

References

1 H. B. Yang, J. Miao, S.-F. Hung, F. Huo, H. M. Chen and B. Liu, *ACS Nano*, 2014, **8**, 10403–10413.
2 J. Huang, K. L. Mulfort, P. Du and L. X. Chen, *J. Am. Chem. Soc.*, 2012, **134**, 16472–16475.
3 C. Gimbert-Suriñach, J. Albero, T. Stoll, J. Fortage, M.-N. Collomb, A. Deronzier, E. Palomares and A. Llobet, *J. Am. Chem. Soc.*, 2014, **136**, 7655–7661.
4 S. Lian, M. S. Kodaimati, D. S. Dolzhnikov, R. Calzada and E. A. Weiss, *J. Am. Chem. Soc.*, 2017, **139**, 8931–8938.
5 M. Liu, M. Liu, X. Wang, S. M. Kozlov, Z. Cao, P. De Luna, H. Li, X. Qiu, K. Liu and J. Hu, *Joule*, 2019, **3**, 1703–1718.
6 S. Lian, M. S. Kodaimati and E. A. Weiss, *ACS Nano*, 2018, **12**, 568–575.
7 B. Chica, J. Ruzicka, H. Kallas, D. W. Mulder, K. A. Brown, J. W. Peters, L. C. Seefeldt, G. Dukovic and P. W. King, *J. Am. Chem. Soc.*, 2020, **142**, 14324–14330.
8 X. J. Wu, S. J. Xie, C. X. Liu, C. Zhou, J. C. Lin, J. C. Kang, Q. H. Zhang, Z. H. Wang and Y. Wang, *ACS Catal.*, 2019, **9**, 8443–8451.
9 Y. S. Jiang, C. Wang, C. R. Rogers, M. S. Kodaimati and E. A. Weiss, *Nat. Chem.*, 2019, **11**, 1034–1040.
10 J. A. Caputo, L. C. Frenette, N. Zhao, K. L. Sowers, T. D. Krauss and D. J. Weix, *J. Am. Chem. Soc.*, 2017, **139**, 4250–4253.
11 S. C. Jensen, S. B. Homan and E. A. Weiss, *J. Am. Chem. Soc.*, 2016, **138**, 1591–1600.
12 Y. Yuan, N. Jin, P. Saghy, L. Dube, H. Zhu and O. Chen, *J. Phys. Chem. Lett.*, 2021, **12**, 7180–7193.
13 C. Huang, X.-B. Li, C.-H. Tung and L.-Z. Wu, *Eur. J. Chem.*, 2018, **24**, 11530–11534.
14 C. Huang, R.-N. Ci, J. Qiao, X.-Z. Wang, K. Feng, B. Chen, C.-H. Tung and L.-Z. Wu, *Angew. Chem., Int. Ed.*, 2021, **60**, 11779–11783.
15 J. K. Widness, D. G. Enny, K. S. McFarlane-Connelly, M. T. Miedenbauer, T. D. Krauss and D. J. Weix, *J. Am. Chem. Soc.*, 2022, **144**(27), 12229–12246.
16 Y. Huang, Y. Zhu and E. Egap, *ACS Macro Lett.*, 2018, **7**, 184–189.
17 Z.-W. Xi, L. Yang, D.-Y. Wang, C.-D. Pu, Y.-M. Shen, C.-D. Wu and X.-G. Peng, *J. Org. Chem.*, 2018, **83**, 11886–11895.
18 Z. Zhang, K. Edme, S. Lian and E. A. Weiss, *J. Am. Chem. Soc.*, 2017, **139**, 4246–4249.
19 C. C. Hewa-Rahinduwage, X. Geng, K. L. Silva, X. Niu, L. Zhang, S. L. Brock and L. Luo, *J. Am. Chem. Soc.*, 2020, **142**, 12207–12215.
20 I. U. Arachchige and S. L. Brock, *J. Am. Chem. Soc.*, 2006, **128**, 7964–7971.
21 J. L. Mohanan, I. U. Arachchige and S. L. Brock, *Science*, 2005, **307**, 397–400.
22 P. R. Brown, D. Kim, R. R. Lunt, N. Zhao, M. G. Bawendi, J. C. Grossman and V. Bulović, *ACS Nano*, 2014, **8**, 5863–5872.
23 A. Pal, I. Ghosh, S. Sapra and B. König, *Chem. Mater.*, 2017, **29**, 5225–5231.
24 C. Landes, C. Burda, M. Braun and M. A. El-Sayed, *J. Phys. Chem. B*, 2001, **105**, 2981–2986.
25 L. Wang, J. Byun, R. Li, W. Huang and K. A. Zhang, *Adv. Synth. Catal.*, 2018, **360**, 4312–4318.
26 J. Luo, B. Hu, W. Wu, M. Hu and T. L. Liu, *Angew. Chem.*, 2021, **133**, 6172–6181.
27 E. H. Discekici, N. J. Treat, S. O. Poelma, K. M. Mattson, Z. M. Hudson, Y. Luo, C. J. Hawker and J. R. de Alaniz, *Chem. Commun.*, 2015, **51**, 11705–11708.
28 E. Zillner, S. Fengler, P. Niyamakom, F. Rauscher, K. Köhler and T. Dittrich, *J. Phys. Chem. C*, 2012, **116**, 16747–16754.
29 M. Micheel, B. Liu and M. Wächtler, *Catalysts*, 2020, **10**, 1143.
30 D. P. Morgan and D. F. Kelley, *J. Phys. Chem. C*, 2018, **122**, 25661–25667.
31 C. Bullen and P. Mulvaney, *Langmuir*, 2006, **22**, 3007–3013.
32 A. McNally, C. K. Prier and D. W. MacMillan, *Science*, 2011, **334**, 1114–1117.
33 M. Schnürch, M. Spina, A. F. Khan, M. D. Mihovilovic and P. Stanetty, *Chem. Soc. Rev.*, 2007, **36**, 1046–1057.
34 H. Kurouchi, *Chem. Commun.*, 2020, **56**, 8313–8316.
35 G. Blasko, V. Elango, B. Sener, A. J. Freyer and M. Shamma, *J. Org. Chem.*, 1982, **47**, 880–885.
36 B. E. Maryanoff and H. R. Almond, *J. Org. Chem.*, 1986, **51**, 3295–3302.